

Connecting field ionization to photoionization via 17- and 36-GHz microwave fields

J. H. Gurian,^{1,*} K. R. Overstreet,¹ H. Maeda,^{1,2,†} and T. F. Gallagher¹

¹*Department of Physics, University of Virginia, Charlottesville, Virginia 22904-0714, USA*

²*PRESTO, Japan Science and Technology Agency, Kawaguchi, Saitama 332-0012, Japan*

(Received 14 October 2009; revised manuscript received 24 June 2010; published 15 October 2010)

Here we present experimental results connecting field ionization to photoionization in Li Rydberg atoms obtained with 17- and 36-GHz microwave fields. At a low principal quantum number n , where the microwave frequency ω is much lower than the classical, or Kepler frequency, $\omega_K = 1/n^3$, microwave ionization occurs by field ionization, at $E = 1/9n^4$. When the microwave frequency exceeds the Kepler frequency, $\omega > 1/n^3$, the field required for ionization is independent of n and given by $E = 2.4\omega^{5/3}$, in agreement with dynamic localization models, which cross over to a Fermi's Golden Rule approach at the photoionization limit. A surprising aspect of our results is that when $\omega \approx 1/2n^2$, the one- and multiphoton ionization rates are similar, and even at the lowest microwave powers, all are 10 times lower than the perturbation theory rate calculated for single-photon ionization. Further, we show that when the Rydberg atoms are excited in the presence of the microwave field, the probability of an atom's being bound at the end of the microwave pulse passes smoothly across the limit. This microwave stimulated recombination to bound Rydberg states can be well described by a simple classical model. More generally, these results suggest that the problem of a Rydberg atom coupled to a high-frequency microwave field is similar to the problem of interchannel internal coupling in multilimit atoms, a problem well described by quantum defect theory.

DOI: [10.1103/PhysRevA.82.043415](https://doi.org/10.1103/PhysRevA.82.043415)

PACS number(s): 32.80.Ee

I. INTRODUCTION

Photoionization of a ground-state atom occurs when the atom is exposed to photons of energy in excess of the ionization potential of the atom, and at low intensities it occurs at a rate proportional to I , the intensity of the radiation. At the other extreme, an electron can be removed from a ground-state atom by field ionization if the saddle point in the combined Coulomb-Stark potential lies below the energy of the ground state. This simple classical picture of field ionization is useful, as tunneling rates increase exponentially with the field. In one case there is a frequency criterion, and in the other, a field criterion. These two extremes are connected by multiphoton ionization, which contains elements of both. For example, N photon ionization requires that N times the photon frequency ω exceeds the ionization potential and the simultaneous absorption of N photons. Since it is an N th-order process, in lowest order perturbation theory it proceeds at a rate proportional to I^N , or E^{2N} , where E is the field amplitude. In practice, the E^{2N} dependence of the ionization rate appears to be very similar to the exponential increase in the field ionization rate with the field.

To connect field ionization to photoionization in a systematic way, one can in principle expose ground-state atoms to fields varying in frequency from 0 to one high enough to effect photoionization. For example, multiphoton ionization of rare gas atoms by 1.06- μm -wavelength radiation occurs essentially by field ionization, whereas multiphoton ionization by 0.53- μm -wavelength radiation, a lower order process, occurs at a substantially lower intensity [1,2]. These

observations show that for ground-state rare gas atoms, 1.06- μm -radiation is low frequency, and ionization occurs by direct field ionization. In contrast, 0.53- μm radiation is no longer low in frequency, and ionization occurs by multiphoton transitions to the ionization continuum.

An alternative approach to connecting field ionization to photoionization is to keep the frequency fixed and alter the initial state of the atom to vary its binding energy, as shown in Fig. 1. At very high n , a microwave photon can photoionize the atom, and photoionization occurs when $\omega > 1/2n^2$. Unless stated otherwise, we use atomic units. At very low n , ionization can be expected to occur by direct field ionization, and at some intermediate n there is a transition from field ionization to multiphoton ionization through higher lying states.

Experiments have shown that for hydrogenlike atoms, the frequency which separates high and low frequency is the $\Delta n = 1$ or Kepler frequency $\omega_K = 1/n^3$, which is the classical orbital frequency of the atomic electron [3]. In particular, experiments have shown that the absolute frequency is not important, only the ratio $\Omega = \omega/\omega_K$, which is usually termed the scaled frequency. For a given frequency ω at low n , $\Omega < 1$ ($\omega < \omega_K$), and the field varies slowly compared to the motion of the electron and has approximately the same effect as a static field. Consequently, ionization of H-like atoms occurs at the field $E = 1/9n^4$. However, as $\Omega \rightarrow 1$ ($\omega \rightarrow \omega_K$) the field required for ionization drops below $E = 1/9n^4$ [4], falling to $E = 0.04/n^4$ at $\omega = \omega_K$ [3,5,6]. The reason for the decreasing field is easily appreciated by examining Fig. 1. Multiphoton transitions to more easily ionized higher n states begin to occur, which allows ionization to occur at lower fields. While the existence of this multiphoton process is obvious, quantum calculations of ionization fields and rates are difficult because there are so many intermediate states, and only recently have such calculations appeared [7]. However, a classical treatment based on the onset of chaos proves to be a very effective way to treat microwave ionization as $\Omega \rightarrow 1$ from below.

*Present address: Laboratoire Aimé Cotton, CNRS, Université Paris-Sud, Bât. 505, F-91405 Orsay, France; jhg8q@virginia.edu

†Present address: Department of Physics and Mathematics, Aoyama Gakuin University, Fuchinobe, Sagami-hara 229-8558, Japan.

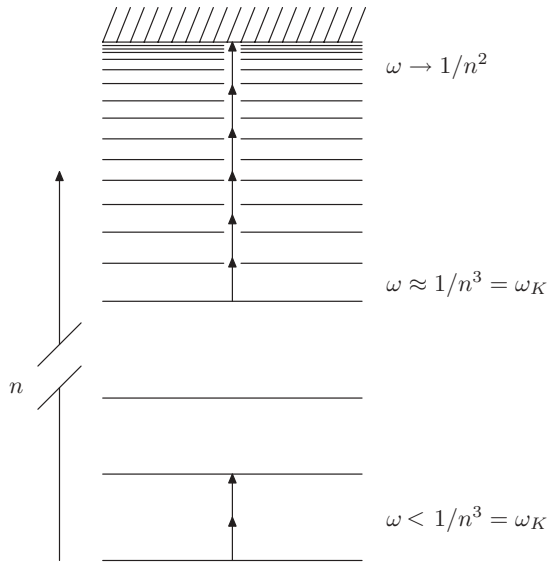


FIG. 1. Energy level diagram of a Rydberg series, with the microwave photon energy shown by arrows. At low n , more than one microwave photon is required to make the $n \rightarrow n + 1$ transition, and for very low n , ionization occurs by field ionization. At very high n , where $\omega > 1/2n^2$, photoionization by a single microwave photon can occur.

One would naturally expect that at higher n , where $\Omega > 1$ ($\omega > \omega_K$), classical mechanics would work increasingly well, and in this regime classical mechanics predicts an ionization field decreasing as $1/n^4$. Instead, a previous experiment using Sr has shown that for $1 < \Omega < 6$, the microwave ionization field is independent of n [8]. An ionization field which is n independent in the $1 < \Omega < 6$ regime is in general agreement with quantum localization models, which have been constructed for H [9–11]. Unlike the $\Omega < 1$ regime [12], for $\Omega > 1$ microwave ionization is predicted to be insensitive to the presence of nonzero quantum defects [7]. In other words, for $\Omega > 1$, microwave ionization of all atoms is predicted to be the same, and the similarity between the Sr experiment and the H calculations supports this prediction. In the regime $1 < \Omega < 6$ the experimental results are in particularly good agreement with the localization model of Jensen [10,11]. The measurements have not, however, tested the range of validity of the localization theory: in particular, how well it works in the photoionization limit, $\omega > 1/2n^2$ or $\Omega > n/2$, where localization theories agree with the perturbation theory result, Fermi's Golden Rule [13].

Here we report the experimental study of the ionization of Li Rydberg atoms by 17.07- and 35.95-GHz microwave fields from $\Omega = 1$ ($\omega = \omega_K$), up to the photoionization limit, $\Omega > 1/2n$ ($\omega > 1/2n^2$). We observed several related results, some of which may be surprising. First, the ionization fields are approximately constant as a function of n or binding energy from $\Omega = 1$ to the ionization limit, although there is obvious structure at the microwave frequency. As a result, the fields required for 10% or 50% ionization by 10 photons are only slightly larger than the analogous fields required for one photon ionization. Second, if the laser excitation occurs in the presence of the microwave field, atoms can be left in bound states even when the laser is tuned above the ionization limit. In other

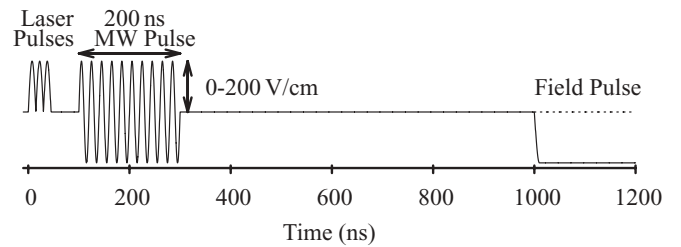


FIG. 2. Experimental timing diagram for the measurement of ionization threshold fields. MW, microwave.

words, stimulated emission by the microwave field recombines the photoelectrons with their parent ions. We interpret both of these phenomena as arising from the strong coupling of the atoms to the microwave field. Finally, we did not find an experimentally accessible regime where Fermi's Golden Rule describes microwave ionization of Rydberg atoms; it is much harder to ionize the atoms than anticipated. In the sections which follow we describe our experimental approach, present the results, compare them to our expectations, and comment on their implications.

II. EXPERIMENTAL APPROACH

A thermal beam of ground-state Li from a resistively heated oven passes through an antinode of a Fabry-Perot microwave cavity, where the atoms are excited by three 20-ns dye laser pulses, via the route $2s \rightarrow 2p \rightarrow 3s \rightarrow np$ for $70 < n < \infty$. We made several kinds of measurements, which require different timing sequences. In Fig. 2 we show the sequence used to measure the microwave ionization fields. As shown in Fig. 2, a 200-ns microwave pulse is injected into the cavity 100 ns after laser excitation. One microsecond after laser excitation a negative voltage is applied to a plate below the cavity to ionize any remaining Rydberg atoms. The resulting electrons pass through a 1-cm-diameter hole in a plate above the cavity and are detected by a dual-microchannel plate detector. The signal from the detector is sent to a gated integrator and recorded by a computer. Electrons produced by photoionization or microwave ionization leave the interaction region before the voltage pulse and are not detected. Stated another way, we detect atoms which have been excited to bound states and survive the microwave pulse. Additional copper plates are placed on either side of the cavity, and bias voltages on the plates and microwave cavity are used to null the stray field in the interaction region to less than 3 mV/cm, as discussed further.

The 17-GHz microwave cavity consists of two brass mirrors of 102-mm radius of curvature separated by 79.1 mm on the horizontal cavity axis. We operate the cavity in the TE_{06} mode at 17.068 GHz with quality factor $Q = 2900$. With this Q the decay or filling time of the energy in the cavity, $\tau = Q/\omega = 27$ ns, sets a lower limit on the pulse length we can use. The microwave source is a Hewlett Packard (HP) 83620A synthesized sweep oscillator. We convert its continuous wave output into pulses using an HP 11720 pulse modulator, and we amplify the pulses with a Hughes 8020H traveling-wave-tube amplifier. The maximum field amplitude we can produce in the cavity is 200 V/cm, and we are able to determine the microwave field with an uncertainty of 8%.

The 36-GHz microwave cavity is constructed of two brass mirrors 40.6 mm in diameter with a 75.9-mm radius of curvature, spaced by 54.2 mm. The cavity is operated in the TE₀₁₀ mode at a frequency of 35.95 GHz with $Q \approx 1600$. The filling time of the cavity is therefore $\tau = 7$ ns. The same HP 83620A synthesized sweep oscillator is used, and it is internally pulse modulated by a transistor-transistor-logic input. The microwave pulses are frequency doubled by a Phase One SP40-2529 frequency doubler and amplified by a Narda DBS-2640X220 amplifier. The amplifier output is sent through a 0- to 50-dB variable attenuator and into the vacuum chamber using a WR-28 waveguide. We can produce 36-GHz microwave fields up to 70 V/cm in amplitude.

The experiment is run at a 1-kHz repetition rate of the frequency-doubled Nd:YLF laser used to pump the dye lasers. Two 20-ns pulses are sliced from the 100-ns-long, 527-nm pump pulse to pump the dye lasers [14]. The $2s-2p$ and $2p-3s$ lasers are of the Littman-Metcalf design [15], and the $3s-np$ laser is a double-grating laser with a linewidth of 5 GHz [16]. Relative frequency measurement of this laser is provided by recording its transmission through a 0.667-cm^{-1} free spectral range etalon, and absolute frequency calibration is provided by recording the optogalvanic signal from the $16274.0212\text{-cm}^{-1}$ $2p^5(2p_{3/2})3s-2p^5(2p_{3/2})2p$ Ne line.

III. OBSERVATIONS

We made three kinds of measurements: microwave ionization fields, single-photon ionization rates, and microwave stimulated recombination.

A. Microwave ionization fields

Since the objective of this work is to connect microwave ionization to photoionization at high n , the focus is on states of high n , where we are not able to resolve individual states within the laser bandwidth. Rather than fix the laser frequency and change the amplitude of the microwave field, we record the field ionization signal of surviving atoms while scanning the $3s-np$ laser frequency for a fixed microwave amplitude and pulse duration. Repeating this procedure for many microwave amplitudes enables us to extract the ionization fields. To ensure the same normalization of the scans the microwave pulse is only turned on for every other laser shot, so each scan provides the survival probability as a function of the binding energy for a specific microwave pulse. Spectra were recorded at 1-dB increments in microwave power, and from the survival probabilities at the same laser frequency and different microwave powers, we extract the 10% and 50% ionization fields.

Data were taken for 200-ns-long, 17.07- and 35.95-GHz microwave pulses, and in Fig. 3(a) we show spectra recorded with six 17-GHz microwave field strengths. With no microwave field we observe resolved bound Rydberg states up to $n \approx 120$ and a flat signal up to 11 GHz below the ionization limit, at which point the signal abruptly drops to 0 since the photoelectrons produced leave before the field ionization pulse in Fig. 2. The signal drops to 0 below the zero-field ionization limit due to the presence of a small residual stray field of 3 mV/cm. Thus the ionization limit in the stray field, or the depressed limit, is 11 GHz below the zero-field

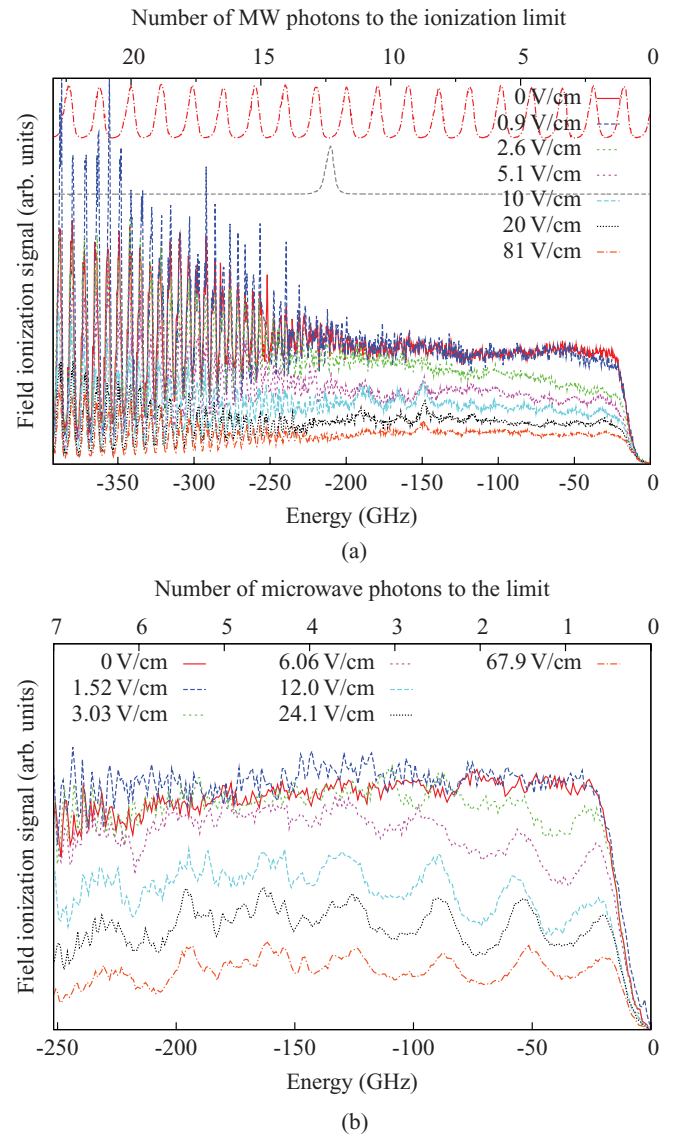


FIG. 3. (Color online) Field ionization signals as a function of laser tuning, given in terms of the binding energy, for 200-ns-long, 17-GHz (a) and 36-GHz (b) microwave (MW) pulses. Etalon signal and optogalvanic signal are also shown in (a). For both 17 and 36 GHz the signals are normalized to the signals obtained with no MW field.

limit. With a microwave field amplitude of 0.9 V/cm there is noticeable, 10%, ionization for laser tunings within 17 GHz, one microwave photon, of the depressed ionization limit and none at lower energies. At this low field, single-photon ionization is observed, but no multiphoton ionization. At 2.6 V/cm there is roughly 30% ionization 17 GHz below the depressed limit and 10% ionization 170 GHz, that is, 10 microwave photons, below the depressed limit. For fields of 5.1 V/cm and greater the fractional ionization is almost independent of the initial binding energy of the atom, although there is an evident 17-GHz modulation in the fraction of atoms which is ionized. In this field regime the ionization probability is the same whether the atom is bound by 10 or 300 GHz. A feature in Fig. 3(a) which we do not understand is why atoms 150 GHz below the limit are particularly resistant to ionization.

In Fig. 3(b) we show scans of the third laser with 200-ns, 36-GHz microwave pulses of several field strengths. The results are qualitatively similar to those shown in Fig. 3(a), the principal difference being the relatively sharper structure at the microwave frequency. At 36 GHz it is apparent that there are peaks in the survival probability located at energies displaced from the depressed ionization limit in the stray field by an integer times the microwave frequency.

By interpolating between spectra, such as those shown in Fig. 3, at each binding energy we determine the threshold fields for 10% and 50% ionization as a function of binding energy, and in Fig. 4 we show the fields at which we observe 10% and 50% ionization for 17 and 36 GHz. The structure

at the microwave frequency shown in Fig. 3 is also apparent in the ionization threshold fields. The peaks in the ionization field are found at the ionization limit in the stray field, modulo the microwave frequency. Apparently atoms at the ionization limit and those which can be brought to it by the absorption of microwave photons are particularly stable. If we ignore the structure in Fig. 4 at the microwave frequency, it is apparent that the ionization fields are n independent and frequency dependent. The observed fields are in excellent agreement with Jensen's localization model, as shown by the dashed lines in Fig. 4. The theory is not expected to reproduce the structures at the microwave frequency. The fact that the Li and Sr experimental ionization fields are the same and match the hydrogenic model confirms the suggestion of Krug and Buchleitner that, for $\Omega > 1$, microwave ionization of all atoms is the same [7]. In Fig. 4(a) we also show the 10% ionization fields for a 500-ns-long, 17.5-GHz pulse calculated by Schelle *et al.* [13], scaled by a factor of $\frac{500}{200}(\frac{17.068}{17.5})^{5/3}$. In their calculations they assumed the bound states to be truncated at $n = 245$, which corresponds to the depression of the limit by a 30-mV/cm field. As shown, their calculated fields reproduce our data very well until one photon below the ionization limit, where they observe essentially complete ionization for Rydberg states, whereas we do not.

B. Photoionization rates

While it is useful to characterize high-order multiphoton ionization by an ionization field, it is more useful to characterize single-photon ionization by a rate, which one could reasonably expect to match the perturbation theory photoionization rate at low microwave power. In other words, it should be given by Fermi's Golden Rule. Accordingly, we measured the population decay due to microwave ionization by a 17-GHz microwave field when we excite atoms to states of $n \sim 430$, 17.07 GHz below the limit. In these measurements we apply a microwave pulse of variable length after laser excitation and observe the number of Rydberg atoms surviving the microwave pulse as a function of its length. Typical results are shown in Fig. 5(a) for a range of microwave field strengths. As shown in Fig. 5(a), for fields in excess of 0.25 V/cm the decays are clearly nonexponential, indicating that photoionization is not the only operative process. In Fig. 5(b) we show the early time decay rates from Fig. 5(a) as well as the calculated decay rates due to photoionization by the 17-GHz microwave fields. Since the Kepler frequency for $n = 430$ is 83 MHz, Fermi's Golden Rule is unlikely to be correct for ionization rates in excess of 10^7 s^{-1} , and for this reason the calculated rate is shown as the dotted line for rates higher than 10^7 s^{-1} . What is surprising is that the observed decay rates are in all cases at least a factor of 5 slower than the computed photoionization rates. For example, at 0.13 V/cm, the lowest microwave field with which we have an observable ionization signal, an approximately exponential decrease in the number of atoms is observed, at the rate of $8.1 \times 10^4 \text{ s}^{-1}$, which differs from the calculated photoionization rate of a Li 430p atom, $4.0 \times 10^5 \text{ s}^{-1}$, by a factor of 5.

Since Rydberg atoms of $n \approx 400$ are very susceptible to small stray static electric fields, it is conceivable that the low photoionization rates shown in Fig. 5 might be due to Stark mixing of angular momentum states, leading to a suppression

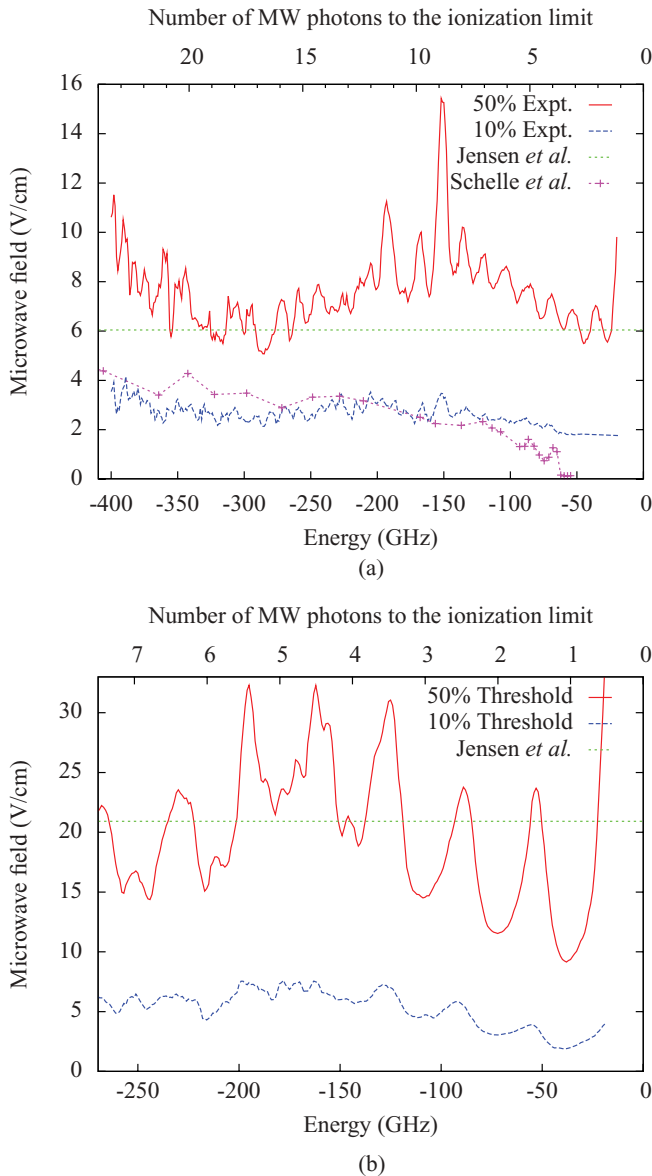


FIG. 4. (Color online) (a) Threshold fields for 10% and 50% microwave (MW) ionization as a function of laser binding energy, for 200-ns-long, 17-GHz pulses, compared to calculated results of Jensen *et al.* [11] and Schelle *et al.* [13]. (b) Threshold 10% and 50% MW ionization fields as a function of binding energy for 200-ns-long, 36-GHz pulses.

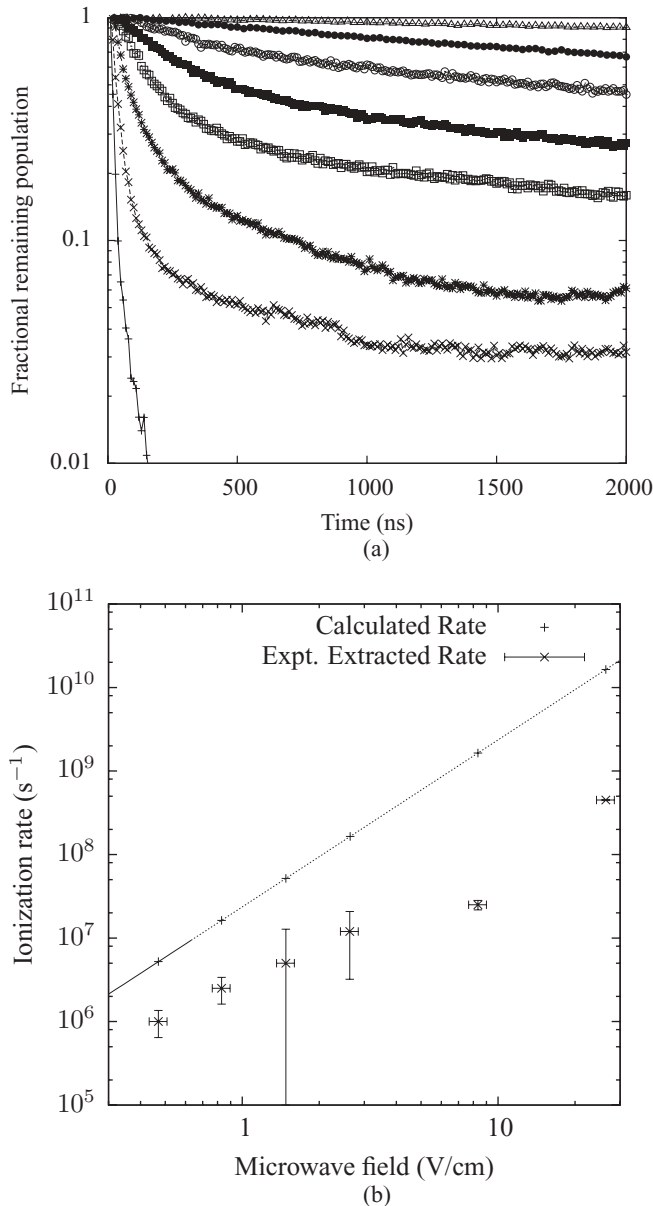


FIG. 5. (a) Fraction of atoms remaining with the laser tuned to 17.045 GHz, i.e., one microwave photon, below the ionization limit as a function of microwave pulse length. The ionization pulse occurs 2500 ns after laser excitation. Data shown are for 17-GHz fields of amplitude 0.13 V/cm (Δ), 0.25 V/cm (\bullet), 0.47 V/cm (\circ), 0.83 V/cm (\blacksquare), 1.48 V/cm (\square), 2.64 V/cm ($*$), 8.34 V/cm (\times), and 26.37 V/cm ($+$). (b) Extracted short-time ionization rates compared to Fermi's Golden Rule predicted rates for microwave fields from 0.47 to 26.37 V/cm. Calculated rates are shown as the dotted line for rates higher than $10^7 s^{-1}$, since we do not expect Fermi's Golden Rule to be valid in this regime.

of the photoionization rate. Accordingly, we measured the amount of microwave ionization as a function of bias fields in all three directions. The most sensitive, by a factor of 10, is the direction in which the microwave field is applied, and in Fig. 6 we show the fraction of atoms surviving a 200-ns-long, 36-GHz pulse as a function of the applied static field for the laser tuned 36 and 54 GHz below the ionization limit. As shown, the ionization is minimized at zero field; a static

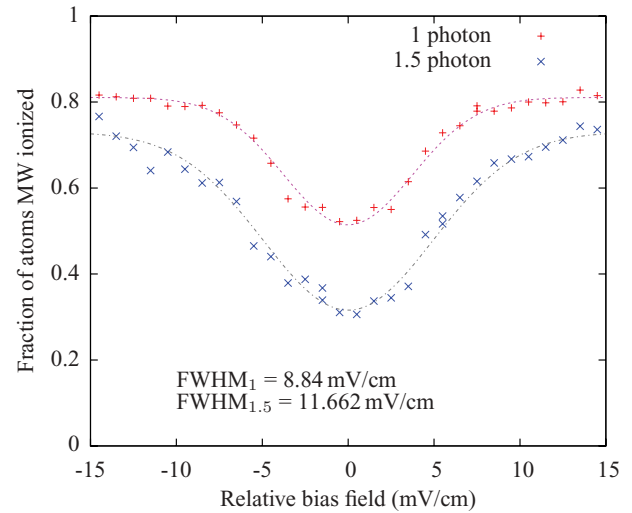


FIG. 6. (Color online) Fraction of atoms ionized by a 200-ns, 5.8-V/cm, 36-GHz microwave (MW) field as a function of external bias field, for laser tunings of 36 and 54 GHz below the ionization limit. These tunings correspond to $n \approx 300$ and $n \approx 247$, respectively. Plotted curves are fitted Gaussians, with FWHM of 8.84 and 11.662 mV/cm, respectively.

field increases the ionization rate. This finding is in complete agreement with the experiments reported by Zhao *et al.* and Yoshida *et al.* [17,18], who found that when the time-average field of a train of pulses is 0, the ionization rate is far lower than when it is nonzero.

The sensitivity of microwave ionization of excited atoms to stray fields provides a simple way to minimize the stray field in the interaction region. Iteratively scanning an applied bias field in each of the three directions to minimize microwave ionization on all three axes enables us to quickly minimize the stray field in the interaction region. Our estimate of 3 mV/cm comes from assigning the depression of the limit to this stray field using $\Delta W = 2\sqrt{E}$.

While the microwave pulse length can be arbitrarily selected using a Stanford Research Systems DG535 digital delay/pulse generator, the rise and fall time of the microwave pulse is limited by the microwave cavity Q . Faster microwave pulse turn-on times can be achieved using a three-port mixer and replacing the microwave cavity with a waveguide or horn [6]. Initial experiments using a WR-28 microwave horn to produce 200-ns-long, 36-GHz pulses with rise and fall times as short as 200 ps exhibit multiphoton ionization resonances similar to those observed using the cavity. Preliminary results indicate that there is no significant difference between results with pulses which turn on or off in 10 cycles and results reported here, for which the pulse was turned on and off in approximately 1000 cycles. This finding is in agreement with previous work by Griffith *et al.* [19], who showed that in a two-level system a pulse turning on in 1 cycle was not very different from one turning on in 1000 cycles. However, a subcycle turn-on introduced an obvious phase dependence.

C. Microwave stimulated recombination

The structure in Fig. 4 at the microwave frequency implies that it is particularly difficult to ionize atoms at the ionization

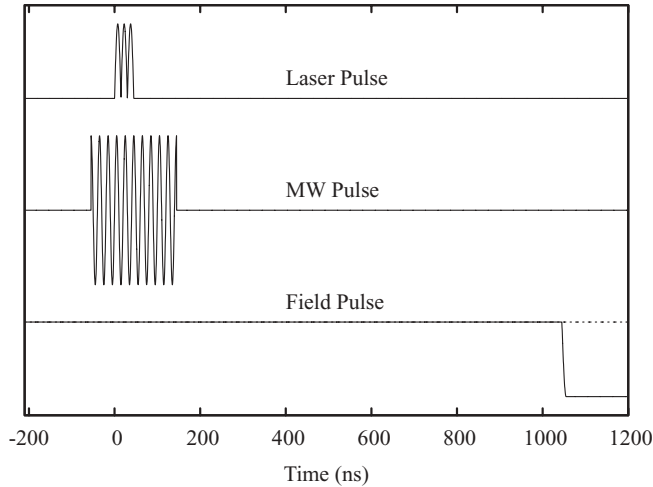


FIG. 7. Experimental timing diagram for laser excitation in the presence of a microwave (MW) field. Laser excitation occurs 100 ns after the start of a 200-ns MW pulse.

limit or atoms which can be brought to the limit by absorption of an integer number of microwave photons. This observation raises the question of whether stable atoms at the limit can be formed by the simulated emission of microwave photons, that is, by the stimulated recombination of a free electron and its parent ion. Since recombination stimulated by a microwave field has been observed by Shuman *et al.* [20], it is reasonable to expect this to be the case. To explore this notion we repeated the experiment shown in Fig. 3 but with the laser excitation occurring in the center of a 200-ns-long microwave pulse and detecting the bound atoms after the microwave pulse, as illustrated in Fig. 7. As shown in Fig. 8, when we scan the wavelength of the third laser we observe a slowly decreasing field ionization signal, which extends smoothly across the limit. In Fig. 8, for example, in the presence of a nonzero microwave field it is not obvious where the limit is. We detect bound atoms at the end of the microwave pulse even when the laser is tuned above the limit. As shown in Fig. 8, similar results are observed for 17 and 36 GHz, although the 36-GHz data are clearer, most likely because the microwave period is shorter so that stray fields have a shorter time in which to disrupt the electron's orbit.

In Fig. 9 we show an expanded view of the 36-GHz data above the ionization limit, which shows that bound atoms are detected even when the laser is tuned 300 GHz above the ionization limit. The data are plotted as a percentage of the atoms which have recombined, assuming that the number of atoms excited is independent of the laser frequency and equal to the number observed just below the limit with no microwaves, as shown in Fig. 9. Each trace is offset vertically by the microwave field at which it was taken, as shown by the scale at the left. Plotting the data in this manner underscores the fact that the extent of recombination is linear in the microwave field amplitude, as observed previously by Shuman *et al.* While the data shown in Fig. 9 appear superficially similar to above-threshold ionization (ATI) [21], they represent the inverse process, the stimulated emission of photons into the microwave field, whereas ATI is due to absorption of photons from the radiation field. The microwave stimulated

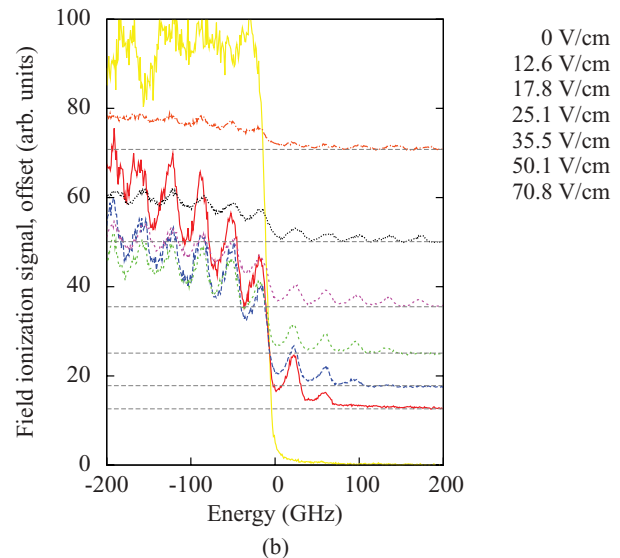
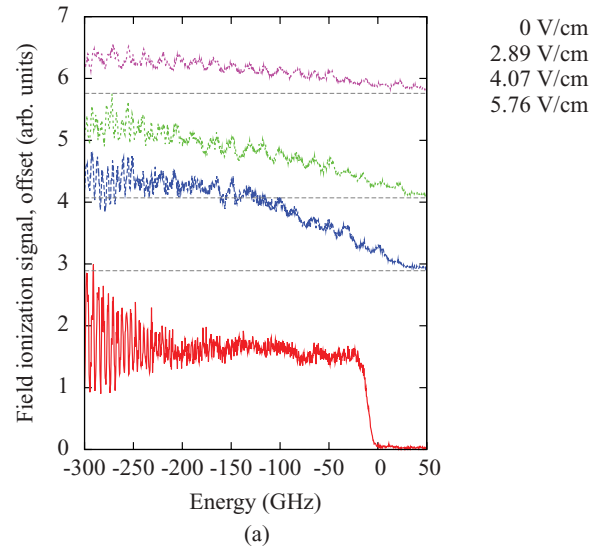


FIG. 8. (Color online) Field ionization signals obtained by scanning the third laser frequency for microwave frequencies of (a) 17 GHz and (b) 36 GHz. The laser excitation occurs during the microwave pulse, and the signal comes from atoms which are bound at the end of the pulse. Zero on the horizontal scale corresponds to laser excitation to the ionization limit. The 17- and 36-GHz signals are normalized to the zero-microwave-field signals. Signals observed with a nonzero microwave field are vertically offset by the microwave field.

recombination we observe is more similar to the laser-assisted Auger decay observed by Schins *et al.* [22].

IV. DISCUSSION

We can extract several useful insights from this work. We consider first the microwave stimulated recombination shown in Figs. 8 and 9. These measurements underscore a point made by Shuman *et al.*: that the presence of the Coulomb potential is important, even in strong radiation fields. One of the standard measures of strong-field phenomena is the ponderomotive energy $U_p = E^2/4\omega^2$, which is the time-average energy of

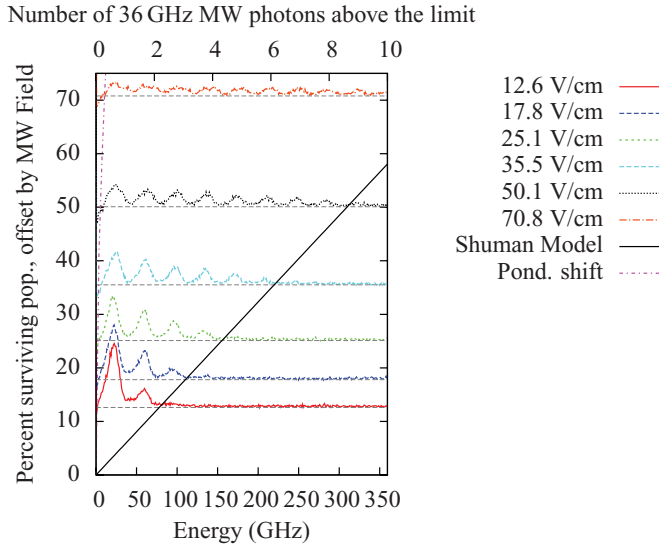


FIG. 9. (Color online) Bound-state atoms resulting from laser excitation above the limit during the 36-GHz microwave (MW) pulse for several MW field amplitudes. The horizontal scale is the third laser tuning above the limit. The vertical scale is the percentage of excited atoms which is detected as bound atoms at the end of the MW pulse. Each trace is offset by its MW field (V/cm), also given by the same vertical scale. The frequency extent of the signals above the limit matches well the energy transfer formula of Shuman *et al.* [solid (black) line], and it is far greater than the ponderomotive shift (magenta dot-dashed line).

oscillation of a free electron in the field $E \cos \omega t$. According to the simpleman's model of ATI, the maximum energy of an electron leaving a strong radiation field is [23–25]

$$W_{\max} = 3U_P = \frac{3E^2}{4\omega^2}. \quad (1)$$

As shown in Fig. 9, this energy is not even close to the extent of the observed microwave stimulated recombination. However, the extent of recombination is almost perfectly matched by [20]

$$W_{\max} = \frac{3E}{2\omega^{2/3}}, \quad (2)$$

as shown by the solid diagonal line in Fig. 9.

The difference between Eq. (2) and the simpleman's model is that Eq. (2) takes into account the fact that the laser excitation creates an electron near the core in the combined potential of the Coulomb field and the microwave field. In contrast, the simpleman's model ignores the Coulomb potential. Due to the fact that the free electron is created near the ion core in the Coulomb potential, it initially has a very high velocity, roughly 1 a.u., and the energy transferred to the electron from the field as it moves away from the core is given by

$$W = - \int_0^{t_f} E(t)v(t)dt. \quad (3)$$

The energy transfer of Eq. (3) is dominated by the first half-cycle of the microwave field, and with suitable approximations the integral in Eq. (3) can be written as Eq. (2) [20].

Probably the two most surprising aspects of these observations are that, with the exception of the weakest microwave

fields, 10-photon ionization is no less likely than 1-photon ionization and that the excitation spectra in Fig. 8 go smoothly across the limit, with obvious structure at the microwave frequency. The experimental results show that the problem does not reduce to Fermi's Golden Rule at the ionization limit. Rather, the problem is dominated by the strong microwave coupling of many bound and continuum levels.

To outline a description of our observations, we begin with the structure at the limit, modulo the microwave frequency, shown in Figs. 8 and 9. The source of the structure is the high- n states at the limit. In these states the Kepler frequency is low and the electron returns to the ion core only infrequently and can only infrequently absorb energy from the field. As a result, high- n states are particularly stable in high-frequency microwave fields. The effect of the microwave field is only to superimpose a fast oscillation at the microwave frequency on the slower orbital motion. Such high-lying states have been observed previously subsequent to exposure of Rydberg atoms to short microwave pulses [26]. More generally, Rydberg states can be found after exposure of atoms to fields far in excess of the static fields required for ionization [27,28]. Since high- n states are stable, it is not surprising that initial states which can absorb or emit microwave photons to reach high- n states are also stable. For this reason we see the peaks in Figs. 8 and 9 displaced from the depressed limit by integer multiples of the microwave frequency. It is clear that there are couplings involving many microwave photons.

Although Jensen's localization model does not reproduce the structure at the microwave frequency shown in Figs. 3 and 4, it does predict the correct average ionization fields for energies to within a few microwave photons of the limit, and it is useful to examine it more carefully. The essence of the model is equating the n -to- n' electric dipole coupling to the average detuning from resonance, so that a chain of many such transitions, extending to the ionization limit, is possible. The n independence of the ionization fields, as shown in Fig. 4, arises from the fact that both the detuning and the matrix element have $1/n^3$ scalings. The matrix element $\langle n|z|n' \rangle$ is given for $|n' - n| > 1$ by [10]

$$\langle n|z|n' \rangle = \frac{0.41}{(nn')^{3/2}\omega^{5/3}}. \quad (4)$$

This matrix element is for a one-dimensional hydrogen atom. The numerical factor is, in general, different for an alkali atom transition, but the functional form is the same [29]. The maximum detuning is given by

$$\Delta\omega = \frac{1}{2n^3}. \quad (5)$$

If $n \cong n' \gg 1$, we may set $n' = n$. Equating the coupling matrix element in the rotating-wave approximation to the average detuning,

$$\langle n|z|n' \rangle \frac{E}{2} = \Delta\omega, \quad (6)$$

yields Jensen's n -independent requirement for ionization, given by

$$E = 2.4\omega^{5/3}, \quad (7)$$

which is shown in Fig. 4 for both 17 and 36 GHz.

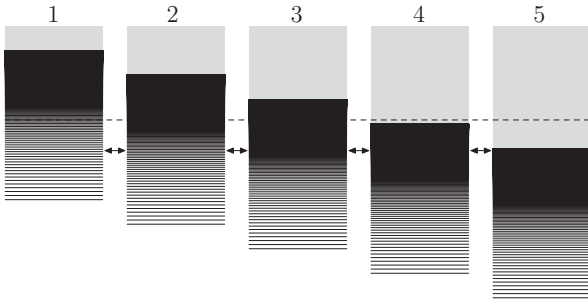


FIG. 10. Floquet picture of Fig. 1. Each Floquet channel is energetically separated from the next channel by one microwave photon. Electric dipole couplings are indicated by the double-headed arrows. As shown by the dashed line, a bound state in channel 3 interacts with the continua in channels 4 and 5 and with more deeply bound levels in channels 1 and 2.

Quantum mechanically the $1/n^3$ scaling of the dipole matrix element comes from the $1/n^{3/2}$ normalization factor of the wave functions, which indicates that only for small z are the n and n' wave functions similar enough to contribute to the matrix element. In simple classical terms the atom can only absorb energy from the high-frequency microwave field when the electron comes close to the core, which happens once per classical orbit, at frequency $1/n^3$. A slightly different way of stating this is that there is a low probability of absorbing a photon each time the orbiting electron scatters from the ion.

The notions of scattering per orbit and multiple n -to- n' couplings suggest that this problem may be amenable to a quantum defect theory approach, and such an approach was employed by Giusti-Suzer and Zoller to describe ATI [30]. The essential idea is as follows. First, the problem is transformed to the Kramers-Henneberger frame [31], which transforms away the oscillatory motion of the electron when it is far from the ion and turns the interaction with the radiation field into an explicitly short-range interaction, with dipole matrix elements having a $1/r^2$ form. The $1/r^2$ form of the matrix elements ensures that, per orbit, the couplings are the same whether they are bound-bound, bound-continuum, or continuum-continuum couplings. Channels of the same ℓ are defined in the usual manner of quantum defect theory, and by adding or subtracting integral numbers of photons to the channels they are converted to Floquet channels.

An energy level diagram for several channels is shown schematically in Fig. 10. Inspection of Fig. 10 reveals that many bound states in channel 3 lie above the ionization limits of channels 4 and 5, as shown by the dashed line in Fig. 10. The coupling between these channels is provided by the Kramers-Henneberger equivalent of the matrix elements in Eq. (4), and as a result, the nominally bound states of channel 2 are autoionizing states. In short, this problem is similar to

the multilimit problems commonly treated by quantum defect theory [32]. It is useful to recall that the interchannel couplings in quantum defect theory are specified on a per-orbit basis, and the matrix element in Eq. (4) is in this form. In the Floquet picture in Fig. 10 the stable states at the ionization limit naturally appear many times, separated by the microwave frequency, just as they do in the experimental results.

An approach which is, in principle, equivalent to the quantum defect theory approach is an interference stabilization model which Fedorov *et al.* applied to the stabilization of Rydberg atoms [33]. Specifically, they considered the possibility of stabilization in high-frequency, high-intensity fields, a notion originally proposed by Gavrilin and Kaminski [34] for ground-state atoms. The calculations of Fedorov *et al.* predict stabilization at high field strengths, which we do not observe. However, their model does not include continuum-continuum coupling, which is included in the quantum defect theory model, as indicated in Fig. 10. The omission of continuum-continuum coupling precludes ATI, and we believe the stabilization to be an artifact of this omission.

While Rydberg atoms appeared to provide an elegant way of connecting photoionization to field ionization, they do not. A Rydberg atom is fundamentally different from a ground-state atom in that it can absorb or emit photons from a radiation field. Furthermore, in experimentally accessible regimes multiple microwave couplings are important, so that it is not possible to observe single-photon ionization in the absence of other processes. Rather, a high- n Rydberg atom in a microwave field is inherently a multichannel problem best described by quantum defect theory.

V. CONCLUSION

In conclusion, we have observed microwave ionization from the n at which the microwave frequency equals the Kepler frequency, $n = 1/\omega^{1/3}$, to the ionization limit, where single-photon microwave ionization is possible. Over this range of n , ionization requires the same average field, although there is structure at the microwave frequency. Excitation in the presence of a microwave field combined with detection of bound atoms results in a spectrum which passes smoothly across the limit. Taken together, these observations suggest that in experimentally accessible regimes, high- n Rydberg states in microwave fields constitute an inherently multichannel problem.

ACKNOWLEDGMENTS

It is a pleasure to acknowledge helpful discussions with R. R. Jones, A. Schelle, A. Buchleitner, D. Delande, E. S. Shuman, and C. H. Greene. This work was supported by National Science Foundation Grant No. PHY-0855572.

- [1] S. Augst, D. Strickland, D. D. Meyerhofer, S. L. Chin, and J. H. Eberly, *Phys. Rev. Lett.* **63**, 2212 (1989).
- [2] A. l'Huillier, L. A. Lompre, G. Mainfray, and C. Manus, *Phys. Rev. A* **27**, 2503 (1983).
- [3] P. M. Koch and K. A. H. van Leeuwen, *Phys. Rep.* **255**, 289 (1995).

- [4] J. E. Bayfield and P. M. Koch, *Phys. Rev. Lett.* **33**, 258 (1974).
- [5] K. A. H. van Leeuwen, G. van Oppen, S. Renwick, J. B. Bowlin, P. M. Koch, R. V. Jensen, O. Rath, D. Richards, and J. G. Leopold, *Phys. Rev. Lett.* **55**, 2231 (1985).
- [6] M. W. Noel, W. M. Griffith, and T. F. Gallagher, *Phys. Rev. A* **62**, 063401 (2000).

- [7] A. Krug and A. Buchleitner, *Phys. Rev. Lett.* **86**, 3538 (2001).
- [8] H. Maeda and T. F. Gallagher, *Phys. Rev. Lett.* **93**, 193002 (2004).
- [9] G. Casati, B. V. Chirikov, D. L. Shepelyansky, and I. Guarneri, *Phys. Rep.* **154**, 77 (1987).
- [10] R. V. Jensen, S. M. Susskind, and M. M. Sanders, *Phys. Rev. Lett.* **62**, 1476 (1989).
- [11] R. V. Jensen, S. M. Susskind, and M. M. Sanders, *Phys. Rep.* **201**, 1 (1991).
- [12] P. Pillet, H. B. van Linden van den Heuvell, W. W. Smith, R. Kachru, N. H. Tran, and T. F. Gallagher, *Phys. Rev. A* **30**, 280 (1984).
- [13] A. Schelle, D. Delande, and A. Buchleitner, *Phys. Rev. Lett.* **102**, 183001 (2009).
- [14] J. H. Gurian, H. Maeda, and T. F. Gallagher, *Rev. Sci. Instrum.* **81**, 073111 (2010).
- [15] M. G. Littman and H. J. Metcalf, *Appl. Opt.* **17**, 2224 (1978).
- [16] M. G. Littman, *Opt. Lett.* **3**, 138 (1978).
- [17] W. Zhao, J. C. Lancaster, F. B. Dunning, C. O. Reinhold, and J. Burgdörfer, *J. Phys. B: At. Mol. Opt. Phys.* **38**, S191 (2005).
- [18] S. Yoshida, C. O. Reinhold, J. Burgdörfer, W. Zhao, J. J. Mestayer, J. C. Lancaster, and F. B. Dunning, *Phys. Rev. A* **73**, 033411 (2006).
- [19] W. M. Griffith, M. W. Noel, and T. F. Gallagher, *Phys. Rev. A* **57**, 3698 (1998).
- [20] E. S. Shuman, R. R. Jones, and T. F. Gallagher, *Phys. Rev. Lett.* **101**, 263001 (2008).
- [21] P. Agostini, J. Kupersztych, L. A. Lompré, G. Petite, and F. Yergeau, *Phys. Rev. A* **36**, 4111 (1987).
- [22] J. M. Schins, P. Breger, P. Agostini, R. C. Constantinescu, H. G. Muller, G. Grillon, A. Antonetti, and A. Mysyrowicz, *Phys. Rev. Lett.* **73**, 2180 (1994).
- [23] H. B. van Linden van den Heuvell and H. G. Muller, in *Multiphoton Processes*, Cambridge Studies in Modern Optics, Vol. 8, edited by S. J. Smith and P. L. Knight (Cambridge University Press, Cambridge, 1988), p. 25.
- [24] T. F. Gallagher, *Phys. Rev. Lett.* **61**, 2304 (1988).
- [25] P. B. Corkum, N. H. Burnett, and F. Brunel, *Phys. Rev. Lett.* **62**, 1259 (1989).
- [26] M. W. Noel, W. M. Griffith, and T. F. Gallagher, *Phys. Rev. Lett.* **83**, 1747 (1999).
- [27] W. E. Cooke, T. F. Gallagher, S. A. Edelstein, and R. M. Hill, *Phys. Rev. Lett.* **40**, 178 (1978).
- [28] T. Nubbemeyer, K. Gorling, A. Saenz, U. Eichmann, and W. Sandner, *Phys. Rev. Lett.* **101**, 233001 (2008).
- [29] J. H. Hoogenraad and L. D. Noordam, *Phys. Rev. A* **57**, 4533 (1998).
- [30] A. Giusti-Suzor and P. Zoller, *Phys. Rev. A* **36**, 5178 (1987).
- [31] W. C. Henneberger, *Phys. Rev. Lett.* **21**, 838 (1968).
- [32] M. Aymar, C. H. Greene, and E. Luc-Koenig, *Rev. Mod. Phys.* **68**, 1015 (1996).
- [33] M. V. Fedorov, M.-M. Tehranchi, and S. M. Fedorov, *J. Phys. B: At. Mol. Opt. Phys.* **29**, 2907 (1996).
- [34] M. Gavrilu and J. Z. Kamiński, *Phys. Rev. Lett.* **52**, 613 (1984).